A&A 452, 1091–1097 (2006)
DOI: 10.1051/0004-6361:20041683

Astronomy & Astrophysics

Effect of Jupiter's mass growth on satellite capture

The prograde case

E. Vieira Neto[1], O. C. Winter[1], and T. Yokoyama[2]

[1] Grupo de Dinâmica Orbital & Planetologia - Unesp, CP 205 CEP 12.516-410 Guaratinguetá, SP, Brazil
e-mail: [ernesto;ocwinter]@feg.unesp.br
[2] Universidade Estadual Paulista - IGCE - DEMAC, CP 178 CEP 13.500-970 Rio Claro, SP, Brazil
e-mail: tadashi@ms.rc.unesp.br

Received 16 July 2004 / Accepted 3 November 2005

ABSTRACT

We study the effects of Jupiter mass growth in order to permanently capture prograde satellites. Adopting the restricted three-body problem, Sun-Jupiter-Particle, we performed numerical simulations backward in time while considering the decrease in Jupiter's mass. We considered the particle's initial conditions to be prograde, at pericenter, in the region $100R_{\mathcal{Q}_+} \leq a \leq 400R_{\mathcal{Q}_+}$ and $0 \leq e \leq 0.5$. The results give Jupiter's mass at the moment when the particle escapes from the planet. Such values give an indication of the conditions that are necessary for capture. An analysis of these results shows that prograde satellite capture is more complex than a retrograde one. It occurs in a two-step process. First, when the particles get inside about $0.85R_{\rm Hill}$ (Hills' radius), they become weakly bound to Jupiter. Then, they keep migrating toward the planet with a strong decrease in eccentricity, while the planet is growing. The radial oscillation of the particles reduces significantly when they reach a radial distance that is less than about $0.45R_{\rm Hill}$ from the planet. Three-dimensional simulations for the known prograde satellites of Jupiter were performed. The results indicate that Leda, Himalia, Lysithea, and Elara could have been permanently captured when Jupiter had between 50% and 60% of its present mass.

Key words. planets and satellites: formation – solar system: formation – solar system: general

1. Introduction

In a previous paper (Vieira Neto et al. 2004), we presented an analysis of the gravitational escape/capture process of retrograde satellites taking the effect of Jupiter's mass growth into account. The analysis indicated the existence of a gravitational capture boundary beyond which a satellite would escape. The numerical simulations presented agreed with that analysis very well. The gravitational capture boundary was determined from the numerical results. It was found that this boundary shows a weak dependence on the time scale of the mass growth. As the time scale increases the boundary seems to converge to one Hill's radius. Given an initial semi-major axis and eccentricity, the results were presented in terms of Jupiter's mass at the moment when the particle escapes from the planet. Such values are an indication of the conditions that are necessary for capture, and they confirm that Jupiter's mass growth is an efficient mechanism for the capture of retrograde satellites.

In the present paper we consider the prograde satellites case to study the gravitational escape/capture process taking the effect of Jupiter's mass growth into account. An analysis of the results shows that prograde satellite capture is more complex than the retrograde one.

In the next section we discuss the change in the zero velocity curves at the Lagrangian point L_1, which is due to the mass variation, and its implications for the capture problem. In Sect. 3, we present our numerical simulations adopting the restricted three-body problem, Sun-Jupiter-Particle, considering the effects of Jupiter's mass growth. The results show at which stage of this growth a given prograde satellite would have been captured. In Sect. 4 we give an explanation for the differences found between the prograde and the retrograde cases. Three-dimensional simulations for the known prograde satellites of Jupiter are presented in Sect. 5, and our final comments are given in the last section.

2. Effects due to mass change

An analysis of the zero velocity curves is a simple way to visualize the likelihood of producing permanent gravitational capture through the mass variation of one of the primaries (Heppenheimer & Porco 1977). We call $C_{\rm J}(L_1)$ the value of the Jacobi constant for the zero velocity curve associated to the inner Lagrangian point L_1. In Fig. 1 we present a curve in the planetocentric $a \times e$ space for a particle at pericenter, whose Jacobi constant at each point equals $C_{\rm J}(L_1)$. In this diagram such curves divide the space into two regions: one to the left of the curve, where trajectories are confined to being around the planet and never escaping, and another to the right of the curve, where trajectories can stay temporarily around the planet, but will sooner or later escape. We call this curve the *critical Jacobi constant curve*.

Figure 1 shows the locations of the critical Jacobi constant curve for the case of Jupiter with its present mass (320 $M_\oplus$) and with 10% of its present mass (32 $M_\oplus$). The area of the region defined by the critical Jacobi constant curve increases with the mass growth, so some trajectories with had $C_{\rm J} < C_{\rm J}(L_1)$ while Jupiter was growing could have $C_{\rm J} > C_{\rm J}(L_1)$ when Jupiter was completely formed. Therefore based only on this simple analysis, the mass accretion mechanism favors to the permanent capture process.

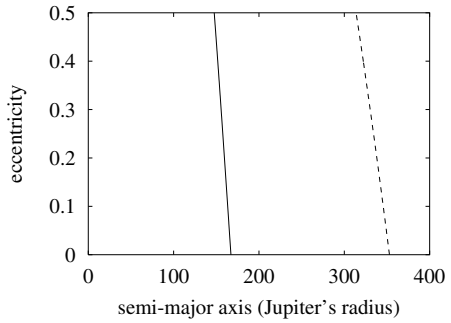

Fig. 1. Critical Jacobi constant curve in the planetocentric $a \times e$ space in opposition at pericenter for a prograde orbit. The curve to the right corresponds to the case of Jupiter with its present mass (320 $M_{\oplus}$), and the left curve corresponds to the case of Jupiter with 10% of its present mass (32 $M_{\oplus}$).

In a system represented by the restricted three-body problem, Sun-planet-particle, the change of the planet's mass produces two important effects on the escape/capture process. One of them is the change of the planet's gravitational sphere of influence. For instance, a planet with increasing mass keeps increasing its Hill's radius,

$$R_{\rm Hill} = \left(\frac{\mu_2}{3}\right)^{\frac{1}{3}} a_{\rm p}, \tag{1}$$

where μ_2 is the reduced mass of the planet and $a_{\rm p}$ its orbital semi-major axis. The other correlated effect produced by the mass variation of the planet is the change in the orbital semi-major axis (a) of its satellites (particles). This change follows the relation given by Jeans (1961)

$$a\mu_2 = \text{constant}. \tag{2}$$

From both Eq. (2) and the conservation of orbital angular momentum during mass loss, one can conclude that the eccentricity is constant, so mass loss cannot directly affect orbital eccentricities.

Since the evolution of the present dynamical system is reversible in time, we preferred to make the analysis go backwards in time. Therefore, we considered a particle that begins as a bound satellite of Jupiter with its present mass, then we follow the dynamical evolution of this particle to the past. As the mass of Jupiter decreases, the semi-major axis of the satellite increases further from the planet (Eq. (2)). As a consequence, the gravitational influence of the planet on the satellite decreases and the perturbation from the Sun increases when the satellite reaches a radial distance from the planet such that its gravitational influence is not enough to keep it bound, and it escapes.

3. Numerical simulations

In order to verify the actual dynamical effects of Jupiter's mass growth on the capture of prograde satellites, we performed some numerical simulations. We considered the planar, circular, restricted three-body problem, Sun-Jupiter-particle, with the linear variation of Jupiter's mass. We integrated backwards in time, i.e., from the present to the past. The particle is initially bound as a satellite of Jupiter with its present mass, then we follow the dynamical evolution of this particle back into the past as the mass of Jupiter decreases. The simulations were interrupted in two situations: i) the 2-body energy, Jupiter-particle, changed from negative to a positive value (escape/capture); ii) the particle collided with Jupiter (collision). From such simulations we determined the time at which the escape occurred for each particle's initial condition. The variation of Jupiter's mass was considered to be linear with time on time scales ranging from 10^2 to 10^5 years. The initial conditions were such that the particles were considered in opposition at pericenter within the ranges $0 \leq e \leq 0.5$ and $100R_{\jupiter} \leq a \leq 400R_{\jupiter}$, where $R_{\jupiter}$ is Jupiter's equatorial radius. Most of the numerical simulations were made considering planar prograde orbits, $I = 0°$.

Assuming that the adopted dynamical system represents the history of this satellite system fairly well, the results found tell us at which stage of Jupiter's mass growth an irregular prograde satellite would have been captured by Jupiter (Fig. 2). The time scale for Jupiter's mass to decrease from its present value to 10% was 10^2 years in Fig. 2a, 10^3 years in Fig. 2c, 10^4 years in Fig. 2e, and 10^5 years in Fig. 2g. Apart from the case of a time scale of 10^2 years, Fig. 2a, the structure of the figures show that the time scale for mass growth is not a very relevant factor for the escape/capture process. We notice that the difference in Jupiter's mass values between the results for two consecutive different time scales decreases as the time scales increases. This is an indication that for longer time scales (10^7, 10^8 years) the results are not very different from those presented here (10^5 years).

The general structures presented in Fig. 2 show that the farther the particle is from the planet the sooner it escapes, as expected. Such a structure means that there is an explicit mutual dependence between the planet's mass, the initial semi-major axis, and eccentricity of the particle. We also note that the dependence on the initial eccentricity is not significant.

In order to better understand the structure shown in Fig. 2, we analyzed a representative set of initial conditions in detail considering the set composed of nine initial conditions given by the combinations of $a = 100R_{\jupiter}$, $200R_{\jupiter}$, $300R_{\jupiter}$, and $e = 0.0$, 0.2, 0.4. The semi-major axis of the orbits evolve as predicted by Jeans' relation (Eq. (2)), as can be seen in the examples presented in Fig. 3. The evolution of the eccentricities can be seen in Fig. 4. As the Jupiter's mass decreases, the amplitude of oscillation of orbit's eccentricities increases, but suddenly they depart from the smooth evolution, and the eccentricities grow to a much higher value until the trajectories become hyperbolic.

The combination of the evolution of the semi-major axis and the eccentricity produces an increase in the orbital radius of the particle and in its amplitude of oscillation. In general, the orbital radius of the particles evolve as shown in the sample given in Fig. 5.

Following the idea that there is a critical distance for the planet, defined as the gravitational capture boundary (Vieira Neto et al. 2004), beyond which the particle will escape, we determined such a boundary from the results of our simulations. In the case of Jupiter's mass-growth time scale of 10^5 years, this boundary is very well fitted by 0.85 Hill's radius, as can be seen in the plots of Fig. 5 (upper dotted lines). In the cases of time scales of 10^4 and 10^3 years, the best fits are $0.84R_{\rm Hill}$ and $0.82R_{\rm Hill}$, respectively. Therefore, the results suggest that the gravitational capture boundary decreases as the mass growth time scale increases, but it also suggests convergence to a value close to $0.85R_{\rm Hill}$.

We also note an anomaly on the eccentricity in Fig. 4, as it shows two different behaviors. First, the oscillation in the eccentricity increases until the semi-major axis reaches approximately $0.45R_{\rm Hill}$. After this point, the eccentricity leaps to higher values. This result is not too far from the prograde stability limit at $0.49R_{\rm Hill}$ found by Hamilton & Burns (1991). Therefore, we

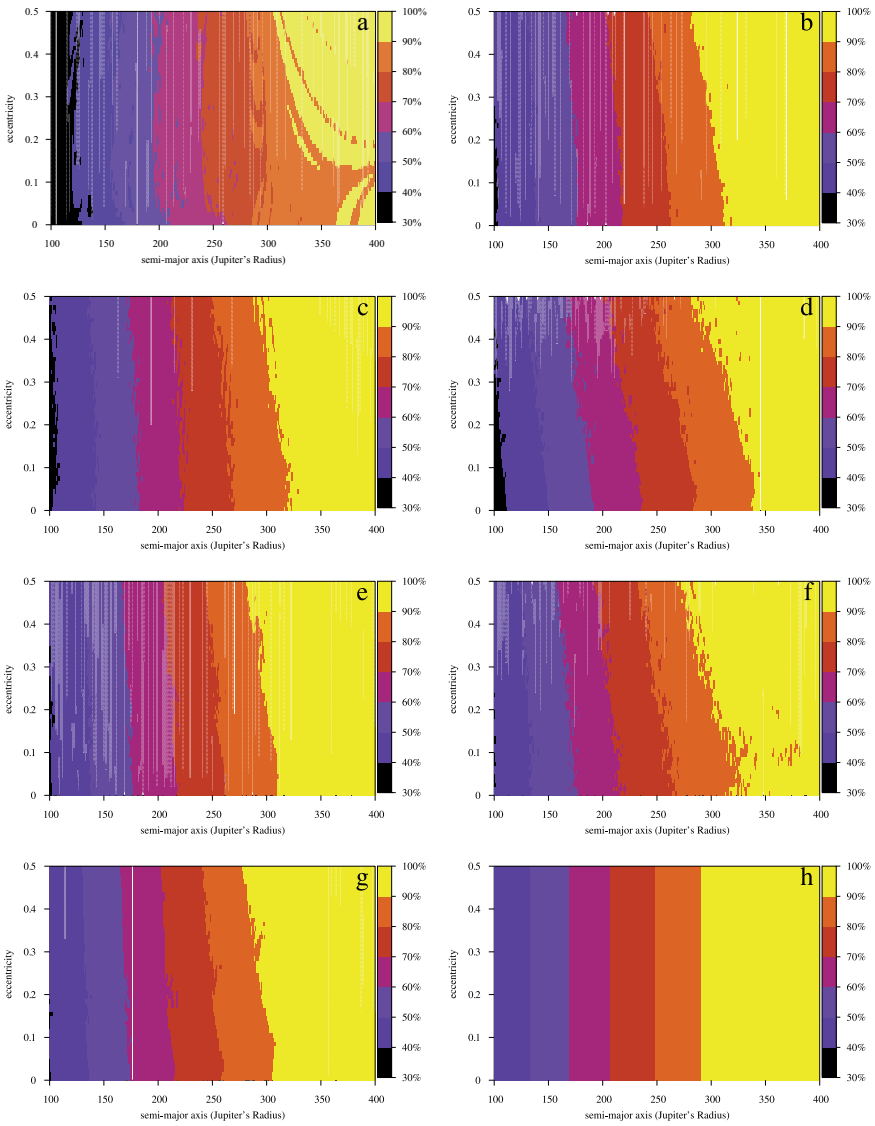

Fig. 2. Mass of Jupiter at the moment of escape for satellites with initial conditions in the planetocentric $a \times e$ space. Initially Jupiter has its present mass (320 $M_{\oplus}$), and the orbits were integrated backward in time with a decreasing mass for Jupiter. In the four figures in the left column, the orbital inclination considered was zero degrees. The time scale for the mass to decrease from its present mass to 10% of its mass was: **a)** 10^2 yr, **c)** 10^3 yr, **e)** 10^4 yr, and **g)** 10^5 yr. There are also three figures where we adopted the time scale 10^5 yr, but with orbital inclinations **b)** 20°, **d)** 40°, and **f)** 60°. The only figure that is not the result of direct numerical integration is **h)**. It presents contour plots given by Eq. (3).

conclude that, for values lower than this limit, the prograde trajectories are stable (permanent capture).

The behavior of the eccentricity is due to a resonance between the longitude of pericenter for the satellite, ϖ, and the location of the Sun, $\lambda_{\odot}$. Such resonance is known as the evection resonance, and its effect on the eccentricity has been studied by Hamilton & Krivov (1997). Figure 6 presents a representative example of the evolution of the resonant argument $\varpi - \lambda_{\odot}$ as a function of the planet's mass, and the evolution of its satellite's eccentricity presented in the first plot of Fig. 4. The jump in the eccentricity occurs while the resonant angle is librating. Therefore, the evection resonance is responsible for destabilizing the satellite.

According to the analysis presented in Sect. 2, at a given stage in the mass evolution of the planet there is a critical radial distance beyond which the satellite escapes. In Fig. 7 we present a diagram of orbital radius versus Jupiter's mass. The plain grey region corresponds to the condition where the object would be orbiting the planet as a permanent satellite, delimited by what we called the *stable gravitational boundary* ($0.45R_{\rm Hill}$). Above that region there is another region, delimited by what we called *weak gravitational boundary* ($0.85R_{\rm Hill}$), where most of the objects would be orbiting the planet as temporary satellites. There is also a line labeled Jean's relation that gives an example of the evolution of the orbital radius as a function of Jupiter's mass. As the mass of the planet changes, the particle's orbital radius goes from inside the region of permanently stable captured to the region of weakly captured, then becomes temporarily captured, and finally escapes to outside, or the other way around, depending on the arrow of the time. Therefore, once the weak gravitational boundary is known, one can identify at which stage of the planet's mass growth a given satellite was captured.

From these results we find that: (*i*) the gravitational boundaries are given as a fraction, α, of the Hill's radius (Fig. 5), i.e. $r^* = \alpha\, R_{\rm Hill} = \alpha\,(\mu_2/3)^{1/3}\, a_{\mathcal{Q}_+}$, where $a_{\mathcal{Q}_+}$ is Jupiter's semi-major axis; (*ii*) the escape/capture of the satellite is almost independent of its initial eccentricity (Figs. 2a–g), i.e. $r^* \simeq a^*$; (*iii*) the semi-major axis evolves according to Jean's relation (Eq. (2) and

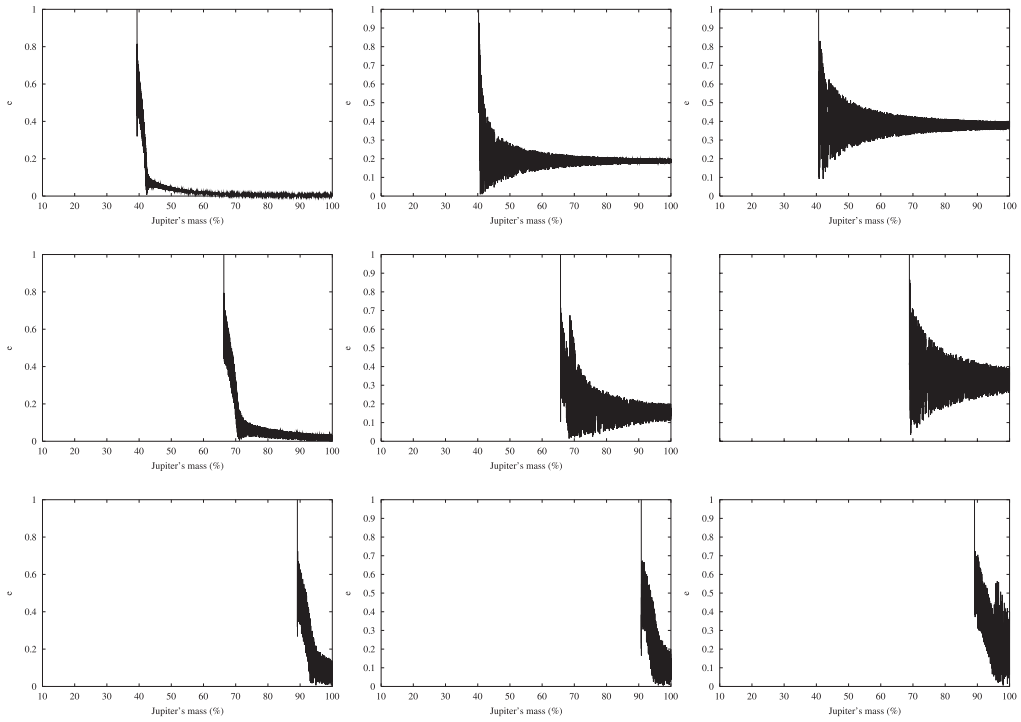

Fig. 4. Evolution of the eccentricity of a sample of satellites as a function of Jupiter's mass. This is a representative sample from the simulations with mass variation time scale equal to 10^5 years. The initial conditions are $a = 100R_{\downarrow}$ (*first row*), $a = 200R_{\downarrow}$ (*second row*) and $a = 300R_{\downarrow}$ (*third row*) with $e = 0.0$ (*first column*), $e = 0.2$ (*second column*) and $e = 0.4$ (*third column*).

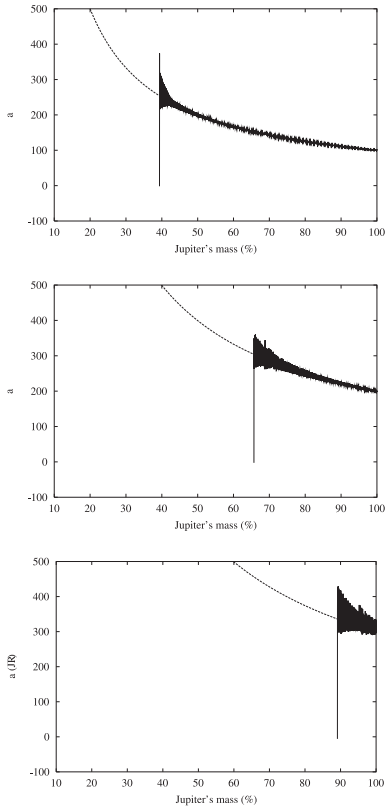

Fig. 3. Evolution of the semi-major axis of a sample of satellites as a function of Jupiter's mass. This is a representative sample from the simulations with mass variation time scale equal to 10^5 years. The initial conditions are: (i) $a = 100R_{\downarrow}$ and $e = 0.0$ (*left*); (ii) $a = 200R_{\downarrow}$ and $e = 0.2$ (*middle*); (iii) $a = 300R_{\downarrow}$ and $e = 0.4$ (*right*). The dashed lines indicate the corresponding values given by Jeans' relation, Eq. (2).

Fig. 3). Then, $a^* = (\mu_{20}/\mu_2)a_0$, where μ_{20} is the reduced mass of Jupiter when it has its present mass. Therefore, the planet's reduced mass, μ_2, at the time the satellite escapes, can be given as a function of the value of the initial semi-major axis, a_0, by

$$\mu_2(a_0) = \left[3\left(\frac{a_0\,\mu_{20}}{\alpha\, a_{\downarrow}}\right)^3\right]^{1/4} . \qquad (3)$$

Adopting the value of the stable gravitational boundary found in our results ($\alpha = 0.45$) in Eq. (3), we computed the mass of Jupiter at the moment of escape for satellites in a grid of semi-major axis and eccentricities. This result is presented in Fig. 2f and is in good agreement with the numerical simulations (Fig. 2g).

4. Prograde versus retrograde

In this section we compare the results shown here for prograde orbits with those for retrograde orbits presented in Vieira Neto et al. (2004).

The size of the incremented region (region between the two curves) shown in Fig. 1 is twice the size of the incremented region produced in the retrograde case (see Fig. 2 of Vieira Neto et al. 2004). Therefore, based on this simple analysis, one could say that this capture mechanism is more efficient for prograde satellites than for retrograde ones. However, this analysis does not tell the whole story. In the retrograde case the convergence of the escape/capture boundary was about $1R_{\rm Hill}$, while in the prograde case the weak gravitational boundary was about $0.85R_{\rm Hill}$ and the stable gravitational boundary is about $0.45R_{\rm Hill}$.

There are two main differences that can be visualized when comparing the semi-major axis versus eccentricity maps for the prograde (Fig. 2) and retrograde (Fig. 5 of Vieira Neto et al. 2004) cases. First, in the prograde case the shifted band does

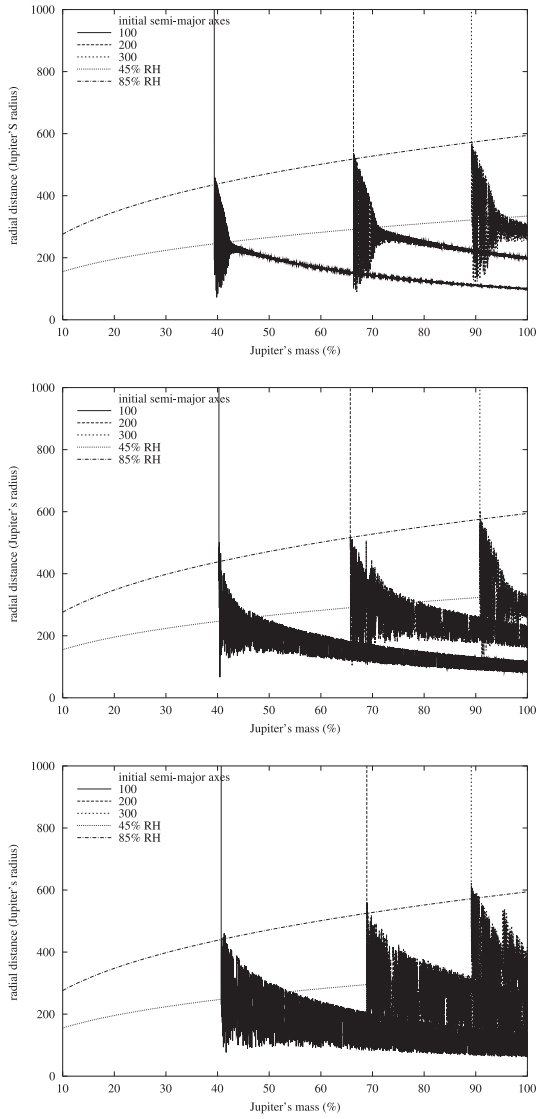

Fig. 5. Evolution of the orbital radius of a sample of satellites as a function of Jupiter's mass. This is a representative sample from the simulations with mass variation time scale equal to 10^5 years. The initial conditions are $a = 100R_{\mathcal{Q}_+}$ (dark gray), $a = 200R_{\mathcal{Q}_+}$ (light gray), and $a = 300R_{\mathcal{Q}_+}$ (black) with $e = 0.0$ (*top*), $e = 0.2$ (*middle*), and $e = 0.4$ (*bottom*). The dotted lines correspond to $85\%R_{\rm Hill}$ and $45\%R_{\rm Hill}$ for the given mass.

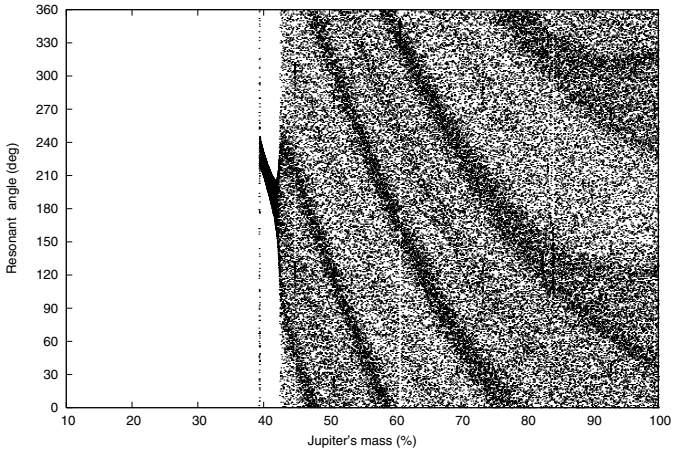

Fig. 6. Evolution of the resonant argument $\varpi - \lambda_\odot$ as a function of the planet's mass for the satellite with initial conditions $a = 100R_{\mathcal{Q}_+}$ and $e = 0$.

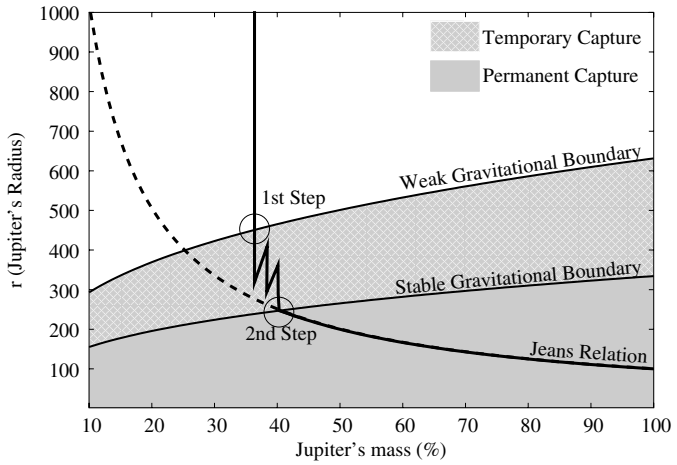

Fig. 7. Diagram of the orbital radius versus Jupiter's mass. The grey area corresponds to the condition where the object would be orbiting the planet as a satellite. The line labeled Jean's Relation gives the evolution of the orbital radius as a function of the mass of Jupiter for an object that would be orbiting as a satellite of Jupiter at the present moment in a circular orbit with $a = 100R_{\mathcal{Q}_+}$. The particle's orbital radius increases while the gravitational capture radius of the planet decreases. The distance at which these two radii coincides is the escape radius.

not appear for low values of eccentricity ($e \leq 0.1$) associated to a family of periodic orbits (Winter & Vieira Neto 2001) that is present in the retrograde case. The effect of this family of periodic orbits decreases as the initial retrograde orbits get far from the plane. This effect almost disappears for orbits when the initial inclination equals 140° (Fig. 5f of Vieira Neto et al. 2004). The second main difference is the dependence on the initial eccentricity. The figures show that there is much less dependence on the eccentricity for the prograde orbits than for the retrograde ones.

A comparison of the evolution of the eccentricities presented here with those given for retrograde orbits (Fig. 6 of Vieira Neto et al. 2004) shows that escape/capture of prograde satellites is more complex than the retrograde ones. It occurs in a two-step process. After remaining fairly flat according to angular momentum conservation, the eccentricity increases abruptly when the particle is captured in the evection resonance.

Since we are interested both in the limits of stability/instability and in its dependence on the eccentricity for prograde and retrograde orbits, we will discuss it into two stages, beginning with considering circular orbits for prograde and retrograde cases. After that we will discuss the effect of the eccentricity in each case.

In Fig. 8 we present two diagrams that indicate velocity vectors for the planet relative to the Sun, $\boldsymbol{V}_{\rm planet}$, and for the satellite relative to the planet, $\boldsymbol{V}_{\rm sat}$, in circular (e = 0) and elliptic orbits (e ≠ 0). Since the time spent by the satellite in the dangerous region near the Lagrange points L_1 and L_2 is a key factor in its escape, our analysis proceeds in terms of the satellite's velocity relative to the Sun. As we are interested in the region where the satellite is more affected by the perturbation of the third body, the discussion will consider the position where the satellite is closest to the Sun.

The modulus of the velocity vector of the satellite in circular orbit, $|\boldsymbol{V}_{\rm sat}|$, is the same for prograde and retrograde orbits. However, the modulus of the satellite velocity relative to the

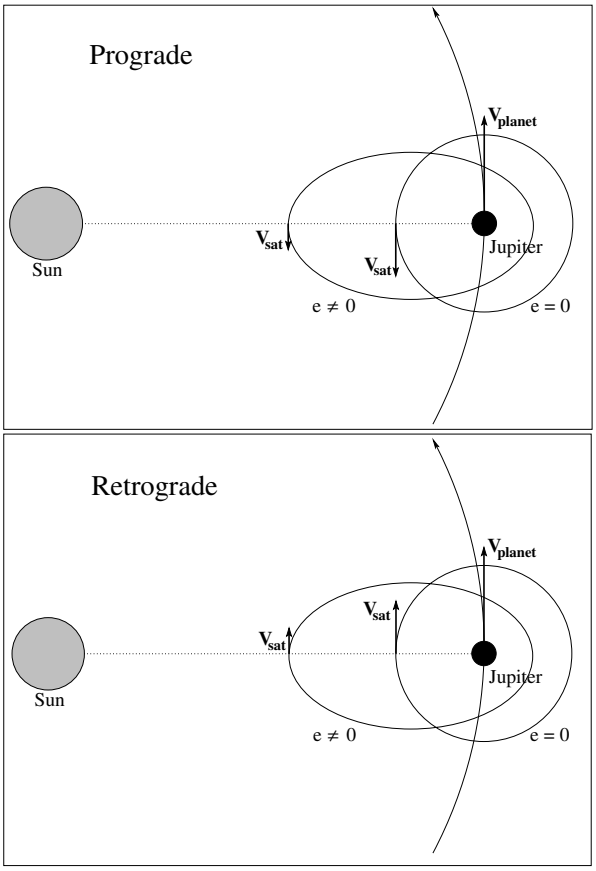

Fig. 8. Schematic diagrams indicating the relative velocities for prograde (*top*) and retrograde (*bottom*) trajectories.

Sun, which plays the role of the perturber, is different from prograde to retrograde in the position considered. In the prograde case it is given by $|\boldsymbol{V}_{\rm planet}| - |\boldsymbol{V}_{\rm sat}| = V_{\rm prog}$, while in the retrograde case it is given by $|\boldsymbol{V}_{\rm planet}| + |\boldsymbol{V}_{\rm sat}| = V_{\rm retrog}$. Therefore $V_{\rm prog} < V_{\rm retrog}$; consequently at a given distance, prograde objects spend more time near the Lagrange points than do retrograde ones. Therefore, they are less stable. This difference can also be explained in terms of the Coriolis acceleration in the rotating reference frame (Hamilton & Burns 1991).

Next we discuss the dependency of the orbit's eccentricity on the velocity of the satellite relative to Sun and the consequence of its perturbation. The diagrams in Fig. 8 show the position of the orbits according to the initial conditions adopted in our simulations. In the case of prograde orbits, we find that at apocenter $V_{\rm prog}$ increases with the increase in the eccentricity, since $|\boldsymbol{V}_{\rm sat}|$ decreases. Therefore, the increased eccentricity allows the orbit to come closer to the Lagrange point but lets it remain there for less time. These effects are a complete contrast. This weak dependency on the eccentricity for objects on prograde orbits can be seen in Fig. 2 and Eq. (3).

In the case of retrograde orbits, the situation is different, since the increase in the eccentricity implies a decrease in $V_{\rm retrog}$. Therefore, the increased eccentricity allows the retrograde orbit to come closer to the Lagrange point and remain there for longer time. This effects accumulate. This dependency on the eccentricity was verified in Fig. 5 and Eq. (4) in Vieira Neto et al. (2004).

Table 1. Orbital elements of the prograde satellites of Jupiter and the stage during Jupiter's mass growth at which the satellites could have been captured (last two columns).

Satellite	a_0	e_0	I_0	Jupiter's mass	
	($R_{\rm J}$)			(10^5 yr)	(10^7 yr)
Themisto	105.00	0.24	43.08°	39%−42%	38%−44%
Leda	156.17	0.16	27.46°	53%−56%	53%−57%
Himalia	160.31	0.16	27.50°	53%−56%	56%−59%
Lysithea	163.89	0.11	28.30°	55%−57%	51%−58%
Elara	164.23	0.22	26.63°	56%−58%	55%−60%
S2000 J11	175.61	0.25	28.30°	52%−61%	61%−63%
S2003 J20	239.19	0.30	55.10°	65%−81%	75%−84%

5. Known prograde satellites

There are seven known prograde irregular satellites of Jupiter. Four of them have been known for more than a quarter of a century (Leda, Himalia, Lysithea, and Elara) and three others were recently discovered: S2003 J2, S2000 J11, and Themisto (Sheppard et al. 2000; Sheppard 2003).

Considering the three-dimensional problem, we numerically simulated the trajectories for sets of initial conditions around their present orbits. The irregular satellites are known to vary their orbits significantly (Saha & Tremaine 1993), so we decided to take their osculating orbital elements at a given epoch, a_0, e_0, and I_0 (Table 1) and used a set of 27 initial conditions for each satellite given by the combinations of $a_0 \pm 0.01a_0$, $e_0 \pm 0.1e_0$, and $I_0 \pm 0.1I_0$. We considered two different time scales for Jupiter's mass-growth, 10^5 and 10^7 years. The Jupiter's mass-growth time scale we considered was 10^5 years.

The results indicate that such satellites could have been captured permanently during Jupiter's mass growth. Table 1 gives the range within which stage of Jupiter's growth should be in order for the capture to occur. Despite the two orders of magnitude difference in the time scales, the ranges of Jupiter's mass values at the time of escape/capture does not change significantly. Following these results, the satellites Leda, Himalia, Lysithea, and Elara could have been captured when Jupiter had between 50% and 60% of its present mass.

6. Conclusions

We have presented an analysis of the gravitational capture/escape process of prograde satellites taking into account the effect of Jupiter's mass growth.

Analysis of our results shows the existence of two boundaries. Inside the inner boundary (stable capture boundary), the satellite is permanently captured with small radial oscillation. Between this boundary and the outer one (weak gravitational boundary), the satellite orbital radius oscillates quite a lot and after some time the satellite is temporarily captured. Beyond the outer boundary the satellite escapes. We showed that between these two radial limits the particles are librating in the evection resonance. Therefore, such resonance seems to be a major step in the process of prograde satellite capture.

The weak gravitational boundary capture was determined from the numerical results. It is found to be 0.85 Hill's radius for a time scale mass growth of 10^5 years, but it gets smaller for shorter time scales.

In the numerical simulation we confirmed that Jupiter's mass growth is an efficient mechanism for the capture of prograde satellites. Our results show at which stage of Jupiter's mass growth a given prograde satellite would have been captured. The actual values, as given in our results, show a dependence on the time scale of the mass growth.

The capture/escape process for prograde trajectories are less dependent on the satellite's eccentricity than for the retrograde ones. The explanation for this is given in terms of the satellite's velocity relative to the Sun.

In the present work we explored the contribution of the planet's mass growth effect alone. Nevertheless, other effects have to be analyzed and combined with the present one in order to indicate the most probable scenario that would have generated irregular satellites. As verified in the previous paper, the contribution of the Galilean satellites and of other giant planets is not relevant in this study.

Acknowledgements. The authors would like to express their thanks to the anonymous referee for suggestions that helped to improve this paper. This work was funded by FAPESP (proc. 02/00344-7) and CNPq, and this support is gratefully acknowledged.

References

Hamilton, D. P., & Burns, J. A. 1991, Icarus, 92, 118
Hamilton, D. P., & Krivov, A. V. 1997, Icarus, 128, 241
Heppenheimer, T. A., & Porco, C. 1977, Icarus, 30, 385
Jeans, J. H. 1961. Astronomy and Cosmogony (New York: Dover)
Saha, P., & Tremaine, S. 1993, Icarus, 106, 549
Sheppard, S. S., Jewitt, D. C., Fernandez, Y., & Magnier, G. 2000, IAUC, 7525
Sheppard, S. S. 2003, IAUC, 8087
Vieira Neto, E., & Winter, O. C. 2001, AJ, 122, 440
Vieira Neto, E., Winter, O. C., & Yokoyama, T. 2004, A&A, 414, 727
Winter, O. C., & Vieira Neto, E. 2001, A&A, 377, 1119
Yokoyama, T., Santos, M. T., Cardin, G., & Winter, O. C. 2003, A&A, 401, 763